Environmental Science Nano

PAPER

View Article Online
View Journal | View Issue

Cite this: *Environ. Sci.: Nano*, 2016, 3, 388

A novel two-compartment barrier model for investigating nanoparticle transport in fish intestinal epithelial cells†

Mark Geppert,‡[a] Laura Sigg[ab] and Kristin Schirmer*[abc]

Received 20th October 2015,
Accepted 25th February 2016

DOI: 10.1039/c5en00226e

rsc.li/es-nano

We introduce a novel *in vitro* rainbow trout intestinal barrier model and demonstrate its suitability for investigating nanoparticle transport across the intestinal epithelium. Rainbow trout (*Oncorhynchus mykiss*) intestinal cells (RTgutGC) were grown as monolayers on permeable supports leading to a two-compartment intestinal barrier model consisting of a polarized epithelium, dividing the system into an upper (apical) and a lower (basolateral) compartment, and thereby mimicking the intestinal lumen and the portal blood, respectively. The cells express the tight junction protein ZO-1 and build up a transepithelial electrical resistance comparable to the *in vivo* situation. Fluorescent polystyrene nanoparticles (PS-NPs; average hydrodynamic diameter: 73 ± 18 nm) were accumulated by RTgutGC cells in a time-, temperature- and concentration-dependent manner. Uptake of PS-NPs was confirmed using fluorescence microscopy. Cells formed an efficient barrier largely preventing the translocation of PS-NPs to the basolateral compartment. Taken together, these data demonstrate the suitability of the *in vitro* barrier model to study the effects of nanoparticles in fish intestinal epithelial cells.

Nano impact

The rapid growth of nanotechnology requires a close investigation of the potential hazardous effects of these new materials not only on humans but also on the ecosystem. Our study introduces the first *in vitro* fish intestinal barrier model based on a rainbow trout intestinal cell line and demonstrates its suitability for studying the role of fish intestinal epithelial cells as a barrier for nanoparticle uptake and transport. We show that nanoparticles can be accumulated in rainbow trout intestinal epithelial cells, but that their transport through the epithelium is largely prevented. The developed model system has great potential in a tiered assessment approach. It can be applied not only for screening particles with respect to their transferability through the fish intestinal epithelium but also for mechanistic investigations of particle effects on the molecular and cellular level.

Introduction

The rapid increase in production, use and release of engineered nanoparticles (ENPs) demands for a thorough investigation of their potential ecotoxicological effects. Considering the aquatic environment, both marine and freshwater systems are known to act as sinks for ENPs as they also do for metals and other environmental pollutants.[1–4] Fish are frequently used model organisms for investigation of the effects of chemicals and ENPs on the aquatic environment. Two major pathways for ENP uptake into fish exist: dietary uptake across the gastro-intestinal system or waterborne uptake across the gill epithelium.[1,5]

Cell lines derived from rainbow trout (*Oncorhynchus mykiss*) are frequently used models for studying the effects of nanoparticles on fish.[6–8] The cell lines used in these studies came from different tissues, such as the gill, gut, liver, brain or gonads. However, none of these studies has explored the barrier potential of rainbow trout intestinal epithelial cells.

The gut of fish is a multifunctional organ not only involved in absorption of nutrients but also in ionic and osmotic regulation.[9] Our current knowledge on this organ comes from *in vivo* and *ex vivo* studies such as the gut sac preparation.[10,11] However, the translocation of ENPs across the gut is poorly understood so far. In an *in vivo* study, Gaiser and co-workers[1] exposed carp (*Cyprinus carpio*) to silver nanoparticles and measured significant increases of silver contents in liver and intestine, suggesting that silver nanoparticles or at least silver ions are being translocated across

[a] *Eawag: Swiss Federal Institute of Aquatic Science and Technology, Environmental Toxicology, Überlandstrasse 133, P. O. Box 611, 8600 Dübendorf, Switzerland. E-mail: kristin.schirmer@eawag.ch*
[b] *ETH Zürich, Institute of Biogeochemistry and Pollutant Dynamics, 8092 Zürich, Switzerland*
[c] *EPF Lausanne, School of Architecture, Civil and Environmental Engineering, 1015 Lausanne, Switzerland*
† Electronic supplementary information (ESI) available. See DOI: 10.1039/c5en00226e
‡ Current address: Department of Molecular Biology, University of Salzburg, 5020 Salzburg, Austria.

the intestinal barrier. Al-Jubory and Handy[12] demonstrated the uptake of titanium across the intestine from TiO_2 nanoparticle exposure by using *ex vivo* statical gut sac preparations and isolated perfused intestines. Although these two exposure systems have their strengths, an *in vitro* cell-line based intestinal barrier model would be a great advantage for detailed investigation of ENP uptake and transepithelial transport, especially with regard to the molecular and cellular mechanisms and for animal-free higher throughput screening. It is therefore our aim to provide the means to investigate the uptake and translocation of ENPs in such a fish intestinal barrier model.

There is a given number of studies describing nanoparticle translocation in the human-derived Caco-2 cell model established by Hidalgo and colleagues.[13] Koeneman and coworkers[14] incubated an intestinal barrier model of Caco-2 cells with TiO_2 nanoparticles and showed that TiO_2 was able to penetrate into and through the cells without disrupting junctional complexes. Similar findings were presented for polystyrene nanoparticles on Caco-2 cells[15] or Caco-2/HT29-MTX co-cultures.[16] In an earlier report, des Rieux and colleagues[17] investigated the transport of polystyrene nanoparticles in a co-culture model of Caco-2, Raji and epithelial microfold cells (M cells[18]). They concluded that the nanoparticle transport by M cells occurs by the transcellular route and is dependent on energy and endocytotic processes.[17] Contrasting results were reported for iron oxide nanoparticles, which were not transported at detectable levels across two different Caco-2 intestinal barrier models.[19] However, it was shown that iron oxide nanoparticles can induce reorganization and distortion of microvilli and disruption of junctions in Caco-2 cells which lead to the loss of epithelial integrity.[20]

We report here the development of a novel two-compartment intestinal barrier model using the rainbow trout intestinal cell line RTgutGC.[21] We show that the model is suitable for investigation of nanoparticle translocation and demonstrate the function of RTgutGC cells as a barrier, which largely prevents translocation of fluorescent polystyrene nanoparticles across the intestinal epithelium.

Materials and methods

Materials

Leibovitz L-15 medium, Versene, CellMask®, 4′,6-diamidino-2-phenylindole (DAPI) and the Alexa Fluor® 488-coupled monoclonal zonula occludens (ZO-1) antibody were purchased from Invitrogen (Basel, Switzerland); fetal bovine serum (FBS) and gentamycin were from PAA (Basel, Switzerland); and trypsin was from Biowest (Nuaillé, France). All other chemicals were from Sigma Aldrich (Buchs, Switzerland) and were of high purity. 75 cm^2 cell culture flasks were obtained from TPP (Transadingen, Switzerland) and 24-well cell culture plates from Greiner-bio-one (Frickenhausen, Germany). Permeable membrane supports with PET-membranes and pore sizes of 0.4, 1 and 3 μm were procured from Greiner-bio-one (Frickenhausen, Germany).

Nanoparticles

Fluoresbrite® carboxylated fluorescent polystyrene nanoparticles (PS-NPs) were purchased from Polysciences (Warrington, PA, United States). These particles have been shown to be suitable for investigation of transepithelial NP transport in an *in vitro* human intestinal barrier model.[16] According to the supplier, the particles appear as 2.5% (25 g L^{-1}) aqueous dispersion containing 3.64×10^{14} particles per mL with a mean particle diameter of 50 nm and a negative surface charge.

Characterization and quantification of PS-NPs

The aqueous PS-NP dispersion was diluted in water or the respective medium (see the ESI† for media description) to a final concentration of 10 mg L^{-1}, and 1 mL of this diluted dispersion was injected into a Malvern DTS-1061 capillary cell (Herrenberg, Germany) and analyzed for hydrodynamic size and zeta potential with a Malvern ZetaSizer Nano ZS (Herrenberg, Germany). Quantification of PS-NPs in media and cell lysates was performed by fluorescence measurement (λ_{ex} = 441 nm, λ_{em} = 486 nm) using a multiwell plate reader (Infinite 2000, Tecan, Maennedorf, Switzerland). The amounts of PS-NPs were calculated from the fluorescence intensities obtained in media/cell lysates compared to the fluorescence intensities obtained in standard curves of PS-NP dilutions in the respective media (see the ESI†).

Cell cultures

Rainbow trout intestinal cells (RTgutGC) were isolated from the gut of a small female rainbow trout as described previously.[21] It has been shown that RTgutGC cells have properties consistent with immortal cell lines and that they are able to be sub-cultured for at least 100 times.[21] For routine culture, RTgutGC cells were kept in 75 cm^2 flasks in complete medium (L-15/FBS, see the ESI†) and incubated at 19 °C under normal atmosphere. Medium change was performed every week. Cells that reached confluency were trypsinized and sub-cultured in a 1 : 3 ratio. For nanoparticle exposure experiments, cells were trypsinized, counted and seeded at a density of 62 500 cells per cm^2 in 300 μL of L-15/FBS in the apical compartment of a permeable membrane support. The basolateral compartment was filled with 1 mL of L-15/FBS and the cells were grown for at least 3 weeks at 19 °C before particle exposure experiments. Medium change of both apical and basolateral media was performed every week. As a control, empty membranes (cell-free) were filled with 300 μL of L-15/FBS (apical chamber) and 1 mL of L-15/FBS (basolateral chamber) and treated identically.

Experimental incubation

Cells were taken out of the incubator and the basolateral and apical media were removed. The cells (apical side) were washed twice with 300 μL of exposure medium (L-15/ex, see the ESI†) before adding 300 μL of L-15/ex containing the desired concentration of PS-NPs. Finally, the basolateral

chamber was re-filled with 1 mL of complete medium (L-15/FBS, see the ESI†) and the cells were incubated in the incubator (19 °C) or fridge (4 °C) for the desired time period. After the incubation, both media were collected and the cells were washed twice with 300 μL of phosphate-buffered saline (PBS). Finally, the cells were lysed by incubating them in 300 μL of 50 mM NaOH for 2 h on a shaker (Geppert *et al.* 2011).[28] Lysates, apical and basolateral media were analyzed for their fluorescence. As controls, cell-free membranes were treated identically.

TEER measurement

Transepithelial electrical resistance (TEER) was measured using an EVOM Voltohmmeter in combination with an Endohm-6 chamber (World Precision Instruments, Berlin, Germany). TEER of RTgutGC cells was calculated by subtracting the blank values (obtained on cell-free membranes) from the values obtained on membranes containing cells.

Fluorescence microscopy

Tight junction staining was performed as follows: cells were taken out of the incubator and washed twice for 5 min with 300 μL of PBS and then fixed for 10 min with 300 μL of 3.7% formaldehyde at 4 °C. Cells were washed twice for 5 min with 300 μL of PBS and then incubated with PBS containing 0.5% Triton X-100 and 5% goat serum for 30 min at 4 °C in the dark. Cells were washed thrice with 300 μL of 0.1% Triton X-100 in PBS for 5 min each and incubated overnight at 4 °C with 100 μL of the primary antibody (Alexa Fluor-coupled ZO-1) in PBS containing 0.5% goat serum and 0.05% Triton X-100. The antibody was used in 1 : 100 dilution. The next day, cells were washed thrice with 300 μL of 0.1% Triton X-100 in PBS for 5 min each and then incubated for 5 min with 300 μL of 10.9 μM DAPI in PBS. After three final washing steps with PBS for 5 min each, the membranes containing the stained cells were cut out of the supports, mounted on microscope slides using the ProLong® Gold antifade reagent (Life Technologies, Carlsbad, CA, United States) and immediately investigated on a Leica SP5 Laser Scanning Confocal Microscope (Leica, Heerbrugg, Switzerland).

Uptake for PS-NPs was investigated using the following protocol: after incubation with PS-NPs, cells were washed thrice with 300 μL of L-15/ex and then incubated for 1 h with 300 μL of 10.9 μM DAPI in L-15/ex in the dark. Cells were washed again with 300 μL of L-15/ex and then incubated for 8 min with 300 μL of 7.5 μg mL^{-1} CellMask® in L-15/ex in the dark. After two additional washing steps with 300 μL of L-15/ex, cells were mounted on microscope slides and investigated immediately by confocal microscopy as described above.

Statistical evaluation

If not stated otherwise, data in figures or tables represent mean value ± standard deviation of three individual experiments, performed with different passages of RTgutGC cells. Pictures of stained cells show representative images of an experiment that was reproduced at least two times with different passages of RTgutGC cells. Statistical analysis of two sets of data was performed using an unpaired *t*-test. Statistical analysis between groups of data was performed using ANOVA with Bonferroni's *post hoc* test. $p > 0.05$ was considered as not significant.

Results and discussion

Nanoparticle characterization

Fluorescent polystyrene nanoparticles (PS-NPs) were used as a model to study the uptake and translocation of nanoparticles in the fish intestinal barrier. These particles were used earlier on Caco-2 cells[16] and have the advantage of being (i) easy to quantify, (ii) non-dissolving and (iii) non-toxic to the cells. According to the supplier, the PS-NPs have a diameter of 50 nm and a carboxylated (negatively charged) surface. The aqueous stock solution of 25 g L^{-1} PS-NPs contained 3.64×10^{14} particles per mL. When diluted to 10 mg L^{-1} (1.456×10^{11} particles per mL) in water, PS-NPs had an average hydrodynamic diameter of 73 ± 18 nm and a zeta potential of −51 ± 1 mV (Table 1). Both values did not significantly change for at least 24 h of incubation, demonstrating the stability of the diluted, negatively charged PS-NPs in water. When diluted in different exposure media (see the ESI† for media composition), PS-NPs form slightly larger agglomerates with a maximum of 166 ± 23 nm determined after 24 h (Table 1). However, PS-NPs still remained in the nanometer range and no precipitation was observed. The zeta potential of PS-NPs diluted in exposure media remained negative, but with lower absolute values than those in water (Table 1). This observation is likely due to the formation of counter ion shells and/or a protein corona around the nanoparticle surface, thereby shielding some of the original negative charge of the PS-NPs.[22,23]

Intestinal barrier model characterization

The rainbow trout intestinal cell line, RTgutGC,[21] was used as a model system for fish intestinal cells. For establishing an intestinal barrier, RTgutGC cells were seeded on permeable membrane supports (Transwell inserts) with pore sizes of 0.4, 1 or 3 μm and grown to confluency, leading to a two-compartment model consisting of an apical (upper) and a basolateral (lower)

Table 1 Characterization of fluorescent polystyrene nanoparticles (PS-NPs)[a]

	Particle diameter (nm)		Zeta potential (mV)	
Medium	1 h	24 h	1 h	24 h
Water	73 ± 18	78 ± 13	−51 ± 1	−54 ± 7
L-15/ex	67 ± 11	120 ± 12	−24 ± 1***	−26 ± 1***
L-15/FBS	72 ± 3	166 ± 23**	−9 ± 1***	−11 ± 1***

[a] PS-NPs were diluted in water, L-15/ex, or L-15/FBS to a concentration of 10 mg L^{-1} and the hydrodynamic diameter and zeta potential were determined 1 and 24 h after dilution. The data represent mean values ± SD of three independent experiments. Asterisks indicate significant differences of values obtained in media samples compared to water. **$p < 0.01$; ***$p < 0.001$.

compartment and a cell monolayer comprising the biological barrier (Fig. 1A and B). The reason for choosing different pore sizes was to evaluate how cell growth is affected by the pores and how the membrane alone (without cells) influences the translocation of PS-NPs by simple diffusion.

Cells developed a transepithelial electrical resistance (TEER) of 33 ± 3 Ω cm^2 (0.4 μm pore size), 30 ± 2 Ω cm^2 (1 μm pore size) or 35 ± 3 Ω cm^2 (3 μm pore size) after 5 weeks of culture (Fig. 1C). These TEER values are much lower than those obtained on the frequently used Caco-2 cell line, which develops a TEER in the range of 500–1000 Ω cm^2 when cultured on permeable membrane supports.[24] According to the classification made by Claude and Goodenough,[25] the epithelium formed by RTgutGC cells has to be considered 'leaky'. Indeed, the TEER of RTgutGC cells is comparable to the TEER values observed in freshly isolated sections of the Atlantic salmon, *Salmo salar*.[26] Cells grow comparatively well on all membranes reaching slightly higher TEER values on membranes with the 3 μm pore size. A possible explanation for this finding is the ability of the cells to migrate through the larger 3 μm pores and thus grow on the other side of the membrane (see the ESI†).

RTgutGC cells grow on all membranes as a monolayer and express the tight junction protein ZO-1 as shown by confocal microscopy (Fig. 1D–F). Thus, all types of membranes investigated were suitable to establish RTgutGC cell monolayers and thereby establish a two-compartment intestinal barrier model. Three weeks were chosen as the minimum culture time for RTgutGC cells before using them for investigation of uptake and translocation of nanoparticles. This decision was made based on the microscopy images and TEER data (Fig. 1C–F), which both demonstrate that the model epithelium has functional properties reflecting the *in vivo* epithelium.

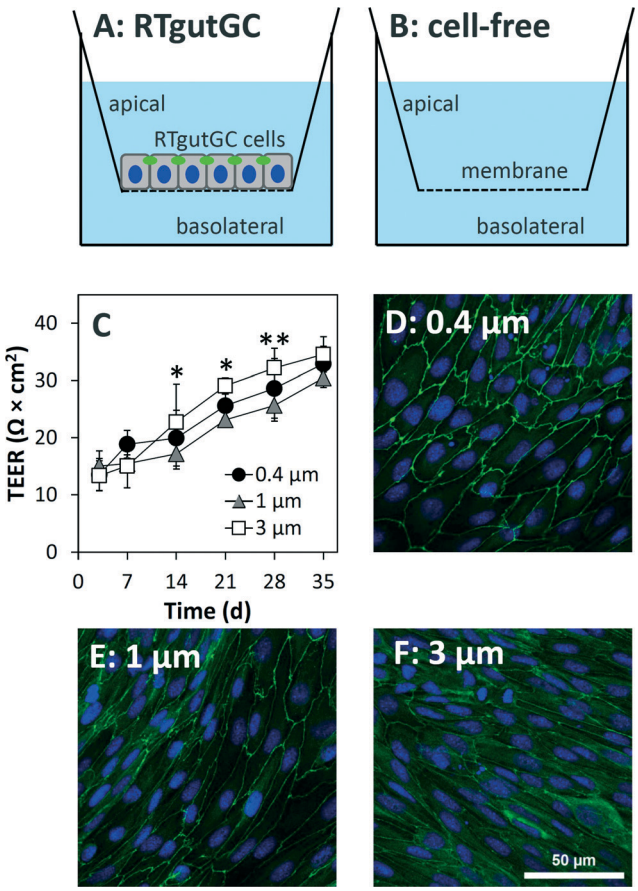

Fig. 1 Characterization of the two-compartment intestinal barrier model. A: Scheme of the two-compartment intestinal barrier model involving rainbow trout intestinal cells (RTgutGC) seeded on permeable membrane supports with different pore sizes (0.4, 1 or 3 μm). B: Empty insert used as cell-free control throughout the experiments. C: Transepithelial electrical resistance (TEER) of the cell epithelium during growth for up to 35 days on membranes with the indicated pore sizes. D–F: Confocal fluorescence microscopy images of RTgutGC cells grown in permeable membrane supports with 0.4 μm (D), 1 μm (E) or 3 μm (F) pore size. The tight junction protein ZO-1 (green) and the nuclei (blue) were stained. The size bar in (F) applies to all images. The data in panel (C) represent mean values ± SD of five to six individual experiments performed on different passages of RTgutGC cells. Asterisks indicate significant differences which were observed between 1 μm and 3 μm pore-size membranes. *$p < 0.05$; **$p < 0.01$.

RTgutGC cells take up PS-NPs but form a barrier for translocation

In order to study the uptake of PS-NPs into RTgutGC cells and the translocation of PS-NPs through the intestinal barrier, the cells were incubated with PS-NPs in exposure medium (L-15/ex) on the apical side and complete medium (L-15/FBS) on the basolateral side. The composition of L-15/ex is very similar to that proposed as a fish gut lumen surrogate,[27] while the serum containing complete medium (L-15/FBS), which was provided in the bottom compartment, mimics the interior facing side of the epithelium. After incubation of RTgutGC cells with 10 mg L^{-1} PS-NPs (4.368 × 10^{10} particles) for 24 h, more than 80% of the applied particles remain in the apical compartment (Fig. 2A). However, RTgutGC cells accumulate between 3.9 and 7.2 × 10^9 particles in the cellular compartment, which accounts for around 9–16% of the total applied PS-NPs (Fig. 2B). Hardly any PS-NPs were detected in the basolateral compartment, indicating that translocation of PS-NPs through the epithelium was very low (Fig. 2C). In order to prove that this is an effect of the cells forming an effective barrier, cell-free membranes were treated identically and PS-NP contents in the different compartments were determined (white bars in Fig. 2). Here, translocation of PS-NPs to the basolateral compartment was detectable for the membranes with 1 and 3 μm pore sizes. For membranes with 3 μm pore size, 8 ± 5 × 10^9 particles translocated to the basolateral compartment which accounts for 18% of the total applied particles. This clearly demonstrates that particle translocation through the membranes is possible and that RTgutGC cells form a barrier, strongly reducing this translocation. It further demonstrates the importance of choosing membranes with appropriate pore sizes that allow the diffusion of nanoparticles to the basolateral compartment.

The findings presented here support the results obtained earlier on iron oxide nanoparticles and Caco-2 cells.[19] However, the results contrast the findings by Koeneman and colleagues who showed that TiO_2 nanoparticles were able to

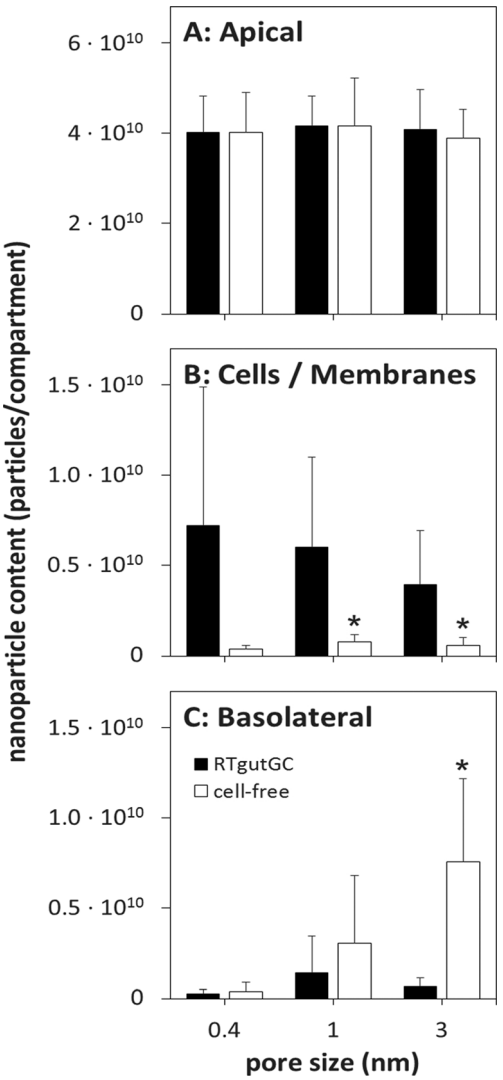

Fig. 2 Uptake and translocation of PS-NPs in the intestinal barrier model. RTgutGC cells were seeded on permeable membrane supports with the indicated pore sizes, grown for three weeks and then incubated with 10 mg L^{-1} PS-NPs for 24 h. After incubation, the apical (A), cellular (B) and basolateral (C) PS-NP contents were determined by fluorescence measurement of the respective media or cell lysates (black bars). As a control, cell-free membranes were treated and analyzed identically (white bars). The data represent mean values ± SD of five experiments performed individually on different passages of RTgutGC cells. Asterisks indicate significant differences which were observed between RTgutGC cells and cell-free conditions. *$p < 0.05$.

penetrate through a Caco-2 intestinal barrier model.[14] This is an interesting result especially considering the fact that Caco-2 cells are known to develop a much tighter epithelium, indicated by higher TEER values (>250 Ω cm^2).[14] However, it has to be noted here that a direct comparison between PS-NPs and metal oxide NPs can be hampered by the fact that ions, potentially released from the metal-based nanoparticles, will be transported differently than the particles themselves. PS-NPs have also been shown to be translocated across Caco-2 monolayers to a very low extent (less than 0.5%,)[15] and Caco-2/HT29-MTX co-cultures to a larger extent.[16] However, it has to be noted that in the second report, M cells are also present in the system which are known to be specialized for transepithelial transport processes.[18]

To further confirm the accumulation of PS-NPs by our fish intestinal barrier model, fluorescence microscopy images were taken after incubation of the cells for 24 h with 100 mg L^{-1} PS-NPs (4.368×10^{11} particles). This higher concentration was chosen in order to achieve a better visualization of PS-NPs in the images. Cell membranes were stained with CellMask® and nuclei were counterstained with DAPI (Fig. 3). Green fluorescence indicated the presence of PS-NPs, which were present as both large and small agglomerates located either as precipitates on the cell layer (white ellipses in Fig. 3A–E) or intracellular (white arrows in Fig. 3B–F) in the perinuclear region. Thus, microscopy clearly supports our hypothesis that RTgutGC cells are able to internalize PS-NPs, probably *via* endocytotic uptake mechanisms as shown earlier for TiO_2 nanoparticles in perfused intestine of rainbow trout.[12]

Concentration, temperature and time dependency of uptake and translocation of PS-NPs

The 3 μm pore-size membranes were chosen to explore the mechanisms of uptake and translocation of PS-NPs in the rainbow trout intestinal barrier model in more detail. After 24 h of incubation of RTgutGC cells with different concentrations of PS-NPs at 19 °C, a concentration-dependent accumulation of particles was observed (Fig. 4C). The maximal amounts of accumulated PS-NPs were $3.8 \pm 0.5 \times 10^{10}$ or $5.6 \pm 0.5 \times 10^{10}$ particles for extracellular exposure concentrations of 30 or 100 mg L^{-1}, respectively. When the incubation was performed at 4 °C, the number of accumulated particles was significantly lower, reaching only $4.6 \pm 0.7 \times 10^9$ (30 mg L^{-1}) or $1.1 \pm 0.2 \times 10^{10}$ (100 mg L^{-1}) particles in the cellular compartment (Fig. 4C). Together with the results from microscopy (Fig. 3), these data strongly corroborate our hypothesis of energy-dependent uptake processes, more specifically endocytosis involved in PS-NP accumulation by RTgutGC cells as shown earlier for different types of NPs on different types of mammalian cells.[15,28,29]

Besides particle accumulation, the amount of translocated PS-NPs to the basolateral compartment was also strongly dependent on the concentration of applied PS-NPs and the incubation temperature (Fig. 4E). After 24 h of incubation, $1.3 \pm 0.2 \times 10^9$ or $3.8 \pm 0.7 \times 10^9$ particles were translocated through the epithelium for exposure concentrations of 30 or 100 mg L^{-1} PS-NPs at 19 °C, respectively. However, these values account only for about 1% of the applied PS-NPs. When the incubation temperature was lowered to 4 °C, the amount of translocated PS-NPs was detectable (detection limit around 1×10^8 particles per mL) only for the highest applied concentration (100 mg L^{-1}) and accounted for $2.8 \pm 0.7 \times 10^8$ particles in the basolateral compartment. In contrast, when empty membranes were incubated with PS-NPs, a concentration-dependent but temperature-independent translocation of particles was measured (Fig. 4F). The TEER of RTgutGC cells did not change during the incubation

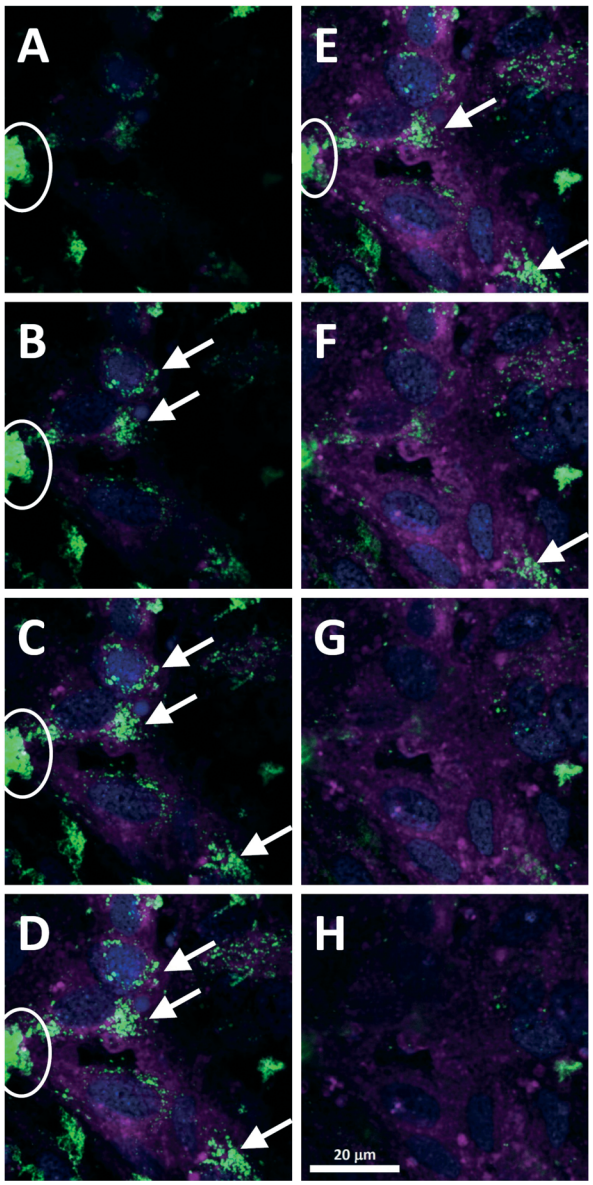

Fig. 3 Internalization of PS-NPs into RTgutGC cells. The cells were seeded on permeable membrane supports (3 μm pore size), grown for three weeks and then incubated with 100 mg L^{-1} PS-NPs for 24 h. After incubation, cell membranes were stained with CellMask® (purple) and nuclei were stained with DAPI (blue). PS-NPs are shown in green and are present as extracellular large agglomerates (white ellipses) or as smaller agglomerates located in the cells (white arrows). Images A–H show a *z*-stack through a representative section of cells with a *z*-distance of 1 μm between the individual images. The size bar in H applies to all panels.

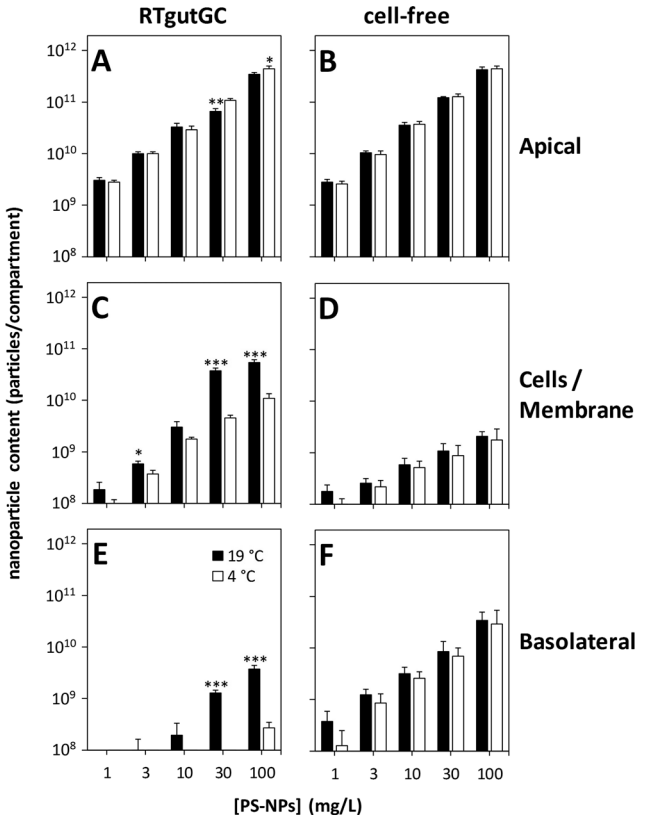

Fig. 4 Temperature and concentration dependency of the uptake and translocation of PS-NPs in the intestinal barrier model. RTgutGC cells were seeded on permeable membrane supports (3 μm pore size), grown for three weeks and then incubated with 1–100 mg L^{-1} PS-NPs for 24 h at 19 °C and 4 °C. After incubation, the apical, cellular and basolateral PS-NP contents were determined by fluorescence measurement of the respective media or cell lysates (A, C, and E). As a control, cell-free membranes were treated and analyzed identically (B, D, and F). The data represent mean values ± SD of three experiments performed individually on different passages of RTgutGC cells. Asterisks indicate significant differences between incubation at 19 °C and at 4 °C (*$p < 0.05$; **$p < 0.01$; ***$p < 0.001$).

with the different PS-NP concentrations, indicating that the integrity of the epithelium is not affected by the incubation conditions (Fig. S3†). Taken together, these results show that the translocation of PS-NPs through the intact epithelial barrier is possible to a low extent when PS-NPs are applied in high concentrations. The temperature dependency of this translocation further supports the hypothesis that energy-dependent processes such as endocytotic uptake of PS-NPs on the apical side and a subsequent release of PS-NPs on the basolateral side are involved.[15]

The hypothesis of active apical uptake and basolateral release of PS-NPs is also supported by the results of the time dependency of PS-NP translocation in RTgutGC cells (Fig. 5). After incubation of RTgutGC cells with 10 mg L^{-1} PS-NPs, translocation of particles was hardly detectable during the first 8 h of incubation, but then it increased to 1.3 ± 1.1 × 10^9, 2.0 ± 0.7 × 10^9 and 4.9 ± 3.5 × 10^9 particles for 24, 72 and 168 h, respectively (Fig. 5E). In parallel, the amount of accumulated PS-NPs in the cells increased strongly, leading to a maximum of 2.6 ± 2.9 × 10^{10} particles after 168 h of incubation (Fig. 5C). This strong accumulation of PS-NPs by the cells, accompanied by the delayed increase in basolateral particle contents, suggests a complex transport mechanism of PS-NPs involving apical uptake and basolateral release of particles.

When empty (cell-free) membranes were incubated with PS-NPs, no further translocation of particles was detectable for incubation times longer than 24 h (Fig. 5F). A possible explanation for this finding could be the formation of larger

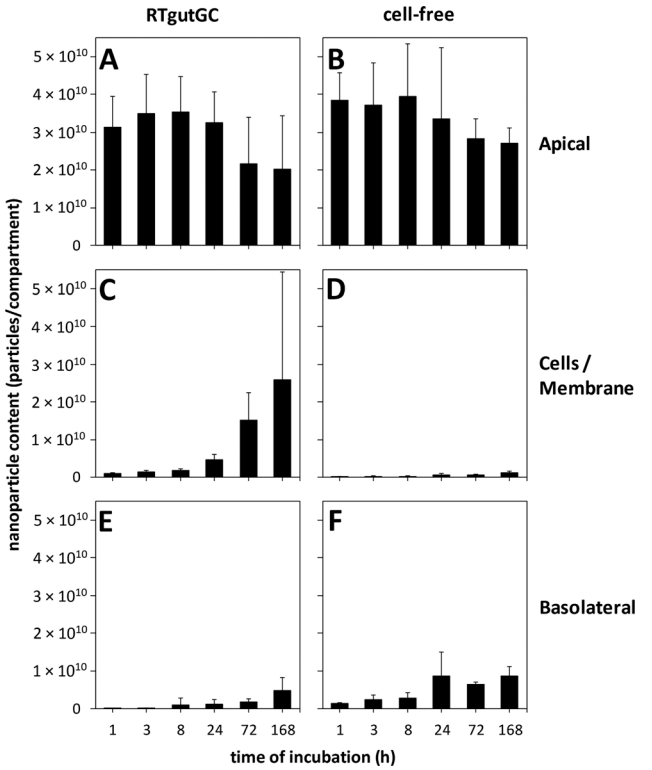

Fig. 5 Time dependency of the uptake and translocation of PS-NPs in the intestinal barrier model. RTgutGC cells were seeded on permeable membrane supports (3 μm pore size), grown for three weeks and then incubated with 10 mg L^{-1} PS-NPs for up to 168 h. After incubation, the apical, cellular and basolateral PS-NP contents were determined by fluorescence measurement of the respective media or cell lysates (A, C, and E). As a control, cell-free membranes were treated and analyzed identically (B, D, and F). The data represent mean values ± SD of three experiments performed individually on different passages of RTgutGC cells.

agglomerates of PS-NPs during the 7 day incubation period. At this time point, particle agglomerates became visible to the eye, which indicates that they are micrometer sized (and therefore out of range of appropriate investigation by DLS measurements). Thus, due to the large size, agglomerates are likely no longer able to penetrate the pores of the membrane. After all, this only occurred in the absence of cells which further supports the hypothesis of an active transport of PS-NPs by the cells.

Conclusions

In conclusion, we present a novel two-compartment intestinal barrier model using the rainbow trout intestinal cell line, RTgutGC, and establish its potential for investigation of nanoparticle translocation through the intestinal epithelium using fluorescent polystyrene nanoparticles (PS-NPs) as a model nanoparticle. RTgutGC cells successfully grow on permeable membrane supports with different pore sizes and we show that the selection of membranes with appropriate pore sizes is a crucial step in developing a model for studying nanoparticle transport. In addition, we demonstrate the barrier function of RTgutGC cells, with the barrier strongly reducing the translocation of PS-NPs to the basolateral compartment. The here presented model is the first *in vitro* model developed from fish cells for studying nanoparticle transport across the intestinal barrier. Its great potential lies in the fact that it can be used for rapid investigation of nanoparticle uptake and translocation in fish intestinal epithelial cells under different experimental conditions. Thus the present model also has potential for high-throughput screening in a tiered testing approach.

Future studies with the model could be designed in a way that further approaches the situation *in vivo*. For example, nanoparticles could be pre-incubated in acidic environments which resemble the situation in the stomach before adding them to the *in vitro* intestinal barrier system. Another approach to advance the model is the use of additional cells like enterocytes in the epithelial layer or fibroblasts seeded on the basolateral side, which will then directly encounter nanoparticles that crossed the epithelium.

Acknowledgements

This research has been supported by EU FP7 grant NanoValid no. 263147. The authors would like to thank Carolin Drieschner and Nadine Bramaz for first establishing ZO-1 staining and Dr. Matteo Minghetti for his help with confocal microscopy.

References

1 B. K. Gaiser, T. F. Fernandes, M. A. Jepson, J. R. Lead, C. R. Tyler, M. Baalousha, A. Biswas, G. J. Britton, P. A. Cole, B. D. Johnston, Y. Ju-Nam, P. Rosenkranz, T. M. Scown and V. Stone, *Environ. Toxicol. Chem.*, 2012, **31**, 144–154.
2 F. Gottschalk, T. Sun and B. Nowack, *Environ. Pollut.*, 2013, **181**, 287–300.
3 K. Schirmer, in *Frontiers of Neuroscience*, ed. J. R. Lead and E. Valsami-Jones, Elsevier, Amsterdam, Netherlands, 2014, vol. 7, pp. 195–221.
4 L. Sigg, in *Comprehensive Water Quality and Purification*, ed. S. Ahuja, Elsevier, Amsterdam, Netherlands, 2014, vol. 4, pp. 315–328.
5 R. D. Handy, G. Al-Bairuty, A. Al-Jubory, C. S. Ramsden, D. Boyle, B. J. Shaw and T. B. Henry, *J. Fish Biol.*, 2011, **79**, 821–853.
6 M. Munari, J. Sturve, G. Frenzilli, M. B. Sanders, A. Brunelli, A. Marcomini, M. Nigro and B. P. Lyons, *Mutat. Res., Genet. Toxicol. Environ. Mutagen.*, 2014, **775–776**, 89–93.
7 N. T. K. Vo, M. R. Bufalino, K. D. Hartlen, V. Kitaev and L. E. J. Lee, *In Vitro Cell. Dev. Biol.: Anim.*, 2014, **50**, 427–438.
8 Y. Yue, R. Behra, L. Sigg, P. Fernández Freire, S. Pillai and K. Schirmer, Role of medium composition on silver nanoparticle toxicity to a fish gill cell line, *Nanotoxicology*, 2015, **9**(1), 54–63.
9 M. Grosell, A. P. Farrell and C. J. Brauner, *The multifunctional gut of fish*, Elsevier, Amsterdam, Netherlands, 2011.

10 R. D. Handy, M. M. Musonda, C. Phillips and S. J. Falla, *J. Exp. Biol.*, 2000, **203**, 2365–2377.
11 I. Hoyle and R. D. Handy, *Aquat. Toxicol.*, 2005, **72**, 147–159.
12 A. R. Al-Jubory and R. D. Handy, *Nanotoxicology*, 2013, **7**, 1282–1301.
13 I. J. Hidalgo, T. J. Raub and R. T. Borchardt, *Gastroenterology*, 1989, **96**, 736–749.
14 B. A. Koeneman, Y. Zhang, P. Westerhoff, Y. Chen, J. C. Crittenden and D. G. Capco, *Cell Biol. Toxicol.*, 2010, **26**, 225–238.
15 B. He, P. Lin, Z. Jia, W. Du, W. Qu, L. Yuan, W. Dai, H. Zhang, X. Wang, J. Wang, X. Zhang and Q. Zhang, *Biomaterials*, 2013, **34**, 6082–6098.
16 G. J. Mahler, M. B. Esch, E. Tako, T. L. Southard, S. D. Archer, R. P. Glahn and M. L. Shuler, *Nat. Nanotechnol.*, 2012, **7**, 264–U1500.
17 A. des Rieux, V. Fievez, I. Theate, J. Mast, V. Preat and Y. J. Schneider, *Eur. J. Pharm. Sci.*, 2007, **30**, 380–391.
18 J. P. Kraehenbuhl and M. R. Neutra, *Annu. Rev. Cell Dev. Biol.*, 2000, **16**, 301–332.
19 B. H. Kenzaoui, M. R. Vila, J. M. Miquel, F. Cengelli and L. Juillerat-Jeanneret, *Int. J. Nanomed.*, 2012, **7**, 1275–1286.
20 W. Zhang, M. Kalive, D. G. Capco and Y. Chen, *Nanotechnology*, 2010, **21**, 355103.
21 A. Kawano, C. Haiduk, K. Schirmer, R. Hanner, L. E. J. Lee, B. Dixon and N. C. Bols, *Aquacult. Nutr.*, 2011, **17**, E241–E252.
22 I. Lynch, A. Salvati and K. A. Dawson, *Nat. Nanotechnol.*, 2009, **4**, 546–547.
23 A. E. Nel, L. Madler, D. Velegol, T. Xia, E. M. Hoek, P. Somasundaran, F. Klaessig, V. Castranova and M. Thompson, *Nat. Mater.*, 2009, **8**, 543–557.
24 E. Liang, K. Chessic and M. Yazdanian, *J. Pharm. Sci.*, 2000, **89**, 336–345.
25 P. Claude and D. A. Goodenough, *J. Cell Biol.*, 1973, **58**, 390–400.
26 K. Sundell, F. Jutfelt, T. Agustsson, R. E. Olsen, E. Sandblom, T. Hansen and B. T. Bjornsson, *Aquaculture*, 2003, **222**, 265–285.
27 J. Genz, A. J. Esbaugh and M. Grosell, *Comp. Biochem. Physiol., Part A: Mol. Integr. Physiol.*, 2011, **159**, 150–158.
28 M. Geppert, M. C. Hohnholt, K. Thiel, S. Nurnberger, I. Grunwald, K. Rezwan and R. Dringen, *Nanotechnology*, 2011, **22**, 145101.
29 C. Petters, F. Bulcke, K. Thiel, U. Bickmeyer and R. Dringen, *Neurochem. Res.*, 2014, **39**, 372–383.